Localized modes in two-dimensional square anisotropic ferromagnets with a hole

Mari Kubota and Kazuko Kawasaki
Department of Physics, Nara Women's University, Nara 630-8506, Japan

Shozo Takeno
Department of Information Systems, Osaka Institute of Technology, Hirakata, Osaka 573-01, Japan

(Received 5 April 1999)

By using the path-integral method with a $SU(2)$ coherent-state basis, two-dimensional anisotropic Heisenberg ferromagnets bearing a fixed magnetic hole are investigated with particular attention paid to interplaying between the intrinsic nonlinearity and the extrinsic structural disorder due to hole doping. Detailed numerical calculations are made for *s*-like localized modes to determine their eigenfrequencies and profiles as a function of a nonlinearity parameter and various anisotropic exchange parameters. A localized magnetic vortex is found in the neighborhood of a hole. Analytical and numerical analyses on their time evolution show two kinds of localized modes separately; one is mobile under certain conditions and intrinsic due to the nonlinearity, and the other is immobile and extrinsic due to the fixed magnetic hole. [S0163-1829(99)01634-3]

I. INTRODUCTION

The effect of dilute impurities on the spin-wave spectrum of ferromagnetic insulators was studied by one of the present authors,[1] and Wolfram and Callaway in 1963,[2] independently. They established the existence of the localized impurity state lying outside of the spin wave. Since then, the subject relating to the localized modes has been extensively developed in several fields, e.g., the antiferromagnetism[3,4] and the lattice vibrations,[5–7] etc. The localized mode concerned so far is due to the extrinsic entities, i.e., spatial inhomogeneity, such as impurity spins or atoms and change in mass, etc.

Recent theoretical development in nonlinear physics, however, reveals the existence of the classical and quantum nonlinear localized modes even in the pure crystal. Anharmonic lattice localized modes,[8–13] which are typical examples for the classical case, appear above the top of the harmonic frequency band of a pure lattice. The quantum nonlinear localized modes are investigated intensively in the Heisenberg magnets.[14–24] They are characterized by the eigenfrequency lying below the bottom of the linear spin wave.

Since the recent discovery of high-T_c superconductor phenomena,[25] the problem of impurity (hole) effect has been revived and received a great deal of attention. As is well known, the parent compounds of high-T_c materials are, in general, antiferromagnetic insulators with considerable high T_N ($\simeq$the room temperature). By increasing hole concentration, T_N decreases dramatically, and finally the magnetic ordering is completely suppressed when the concentration exceeds a certain critical value. On the other hand, the superconducting appears at the opposite condition. Namely, the magnetic ordered phase and the superconducting phase never coexist. So, it becomes now one of the most important problems how the phase transition occurs from magnetic ordered phase to superconducting phase (vice versa) via hole doping.

It is the purpose of this paper to make a detailed and quantitative study on the interplay between intrinsic nonlinearity and extrinsic spatial discreteness due to hole doping during the formation of the localized mode and consider the relation between the appearance of the localized mode and magnetic disorder. We are actually concerned here with moving localized modes as well as the stationary ones for a two-dimensional (2D) Heisenberg ferromagnet containing a fixed magnetic hole. As for the antiferromagnetic case, we will discuss that in a subsequent paper.

The present authors have previously formulated a $SU(2)$ coherent state path-integral theory of nonlinear self-localized collective modes.[15] As mentioned before, this formalism has the following features. (i) No assumption is made on the smallness of spin deviation from the ordered state to make full inclusion of the intrinsic nonlinearity in the magnon system. (ii) To derive a nonlinear differential-difference equation for collective modes, a stationary-phase approximation is employed. In this sense, the formalism corresponds to the classical approach. (iii) No continuum approximation for the lattice is allowed. By employing this formulation to 1D anisotropic Heisenberg ferro- and antiferromagnets, which are spatially homogeneous, we showed interesting features of nonlinear self-localized modes.[14–16,21,23] Therefore our task here is an extension of the theory to 2D magnon system to treat both extrinsic and intrinsic factors simultaneously. This paper is organized as follows: In the next section, a brief account is given of $SU(2)$ coherent-state path-integral formulation to derive discrete and nonlinear differential-difference equations for complex spin-deviation field variables. In Sec. III, the eigenvalue equation of the stationary localized mode is derived for 2D square ferromagnets containing a fixed hole. By introducinging two different magnon Green's functions, one of which is associated with the pure system without nonlinear effect and the other with a linear but spatially inhomogeneous system, the energy eigenvalue is obtained numerically. The profiles of the stationary localized modes are also examined. In Sec. IV, numerical calculation with the Runge-Kutta-Jill method[26] is carried out for the time-evolution equation for the localized modes, and two kinds of localized modes are illustrated separately, i.e., one is intrinsic due to nonlinearity and mobile under certain conditions, and the other is extrinsic due to fixed magnetic hole and immobile. The last section is devoted to concluding remarks of results obtained in this paper.

II. *SU*(2) COHERENT-STATE PATH-INTEGRAL FORMULATION AND STATIONARY PHASE APPROXIMATION

We consider Heisenberg ferromagnets on a 2D square lattice with the lattice constant $a=1$. The Hamiltonian can be written in the form

$$H=-\sum_{\langle nm\rangle} J(n,m)[\eta(S_n^+S_m^-+S_n^-S_m^+)+S_n^zS_m^z], \quad 0<\eta<1, \tag{1}$$

where the symbol $\Sigma_{\langle nm\rangle}$ indicates pairs of nearest neighbors. The quantity $S_n^\alpha(\alpha=x,y,z)$ with $S_n^\pm=S_n^x\pm iS_n^y$ is the α component of the nth site spin operator situated on the lattice vector

$$\boldsymbol{n}=n_1\boldsymbol{e}_1+n_2\boldsymbol{e}_2. \tag{2}$$

Here, n_j ($j=1$ or 2) takes an integer value and $\boldsymbol{e}_j$ denotes an unit vector of jth component. The quantities $J(n,m)>0$ and η are the exchange interaction constant between neighboring sites n and m and its anisotropic parameter, respectively.

Let $|S,M\rangle_n$ be angular-momentum eigenstates of a single spin S_n with spin magnitude S, where $M(=-S,-S+1,\ldots,S-1,S)$ is the eigenvalue of S^z. Then, $SU(2)$ coherent states $|\mu_n\rangle$ associated with the spin S_n are defined by[27–29]

$$|\mu_n\rangle=(1+|\mu_n|^2)^{-S}\exp(\mu_nS_n^+)|S,-S\rangle_n, \tag{3}$$

where the μ_n's are complex magnon field variables. The diagonal coherent-state representations of the spin operator $\boldsymbol{S}_n$ are given by

$$\langle\mu_n|S_n^+|\mu_n\rangle=2S\frac{\mu_n}{1+|\mu_n|^2},$$

$$\langle\mu_n|S_n^-|\mu_n\rangle=2S\frac{\mu_n^*}{1+|\mu_n|^2},$$

$$\langle\mu_n|S_n^z|\mu_n\rangle=S\frac{1-|\mu_n|^2}{1+|\mu_n|^2}. \tag{4}$$

The coherent state $|\Lambda\rangle$ of the whole spins constituting this ferromagnet is defined as

$$|\Lambda\rangle=\prod_n|\mu_n\rangle. \tag{5}$$

As is well known in the path-integral theory,[30,31] the functional integral representation for the matrix element of the evolution operator $\exp(-iHt/\hbar)$ between an initial state $|\Lambda_i\rangle\equiv|\Lambda(t_i)\rangle$ and a final state $|\Lambda_f\rangle\equiv|\Lambda(t_f)\rangle$ can be written in the form[29,31]

$$\langle\Lambda_f|\exp[-iH(t_f-t_i)/\hbar]|\Lambda_i\rangle=\int\mathcal{D}(\Lambda)\exp(iS/\hbar), \tag{6}$$

with

$$S=\int_{t_i}^{t_f}L\,dt\equiv\int_{t_i}^{t_f}\mathcal{L}(\Lambda,\dot{\Lambda},\Lambda^*,\dot{\Lambda}^*)dt, \tag{7}$$

in which

$$\mathcal{L}=\sum_n\frac{S}{1+|\mu_n|^2}\left[\mu_n^*i\hbar\frac{d\mu_n}{dt}-\mu_ni\hbar\frac{d\mu_n^*}{dt}\right]-\langle\Lambda|H|\Lambda\rangle. \tag{8}$$

The functional integration involving the symbol $\mathcal{D}(\Lambda)$ in Eq. (6) means a sum over all paths moving forward in time t. An explicit expression for $\langle\Lambda|H|\Lambda\rangle$ in Eq. (8) is given by

$$\langle\Lambda|H|\Lambda\rangle=-S^2\sum_{\langle nm\rangle}J(n,m)\times\frac{2\eta(\mu_n^*\mu_m+\mu_n\mu_m^*)+(1-|\mu_n|^2)(1-|\mu_m|^2)}{(1+|\mu_n|^2)(1+|\mu_m|^2)}. \tag{9}$$

As a first-order approximation to the exact path-integral formalism described above, we employ the saddle-point approximation to Eq. (6):

$$\delta S\equiv\delta S(\Lambda,\Lambda^*)=0, \tag{10}$$

then the Lagrange equations are obtained as

$$\frac{d}{dt}\left(\frac{\partial\mathcal{L}}{\partial\dot{\mu}_n}\right)-\frac{\partial\mathcal{L}}{\partial\mu_n}=0 \quad \text{and c.c.} \tag{11}$$

Combining Eq. (8) with Eq. (11) gives

$$i\hbar\frac{d\mu_n}{dt}=\frac{(1+|\mu_n|^2)^2}{2S}\frac{\partial\langle\Lambda|H|\Lambda\rangle}{\partial\mu_n^*} \quad \text{and c.c.} \tag{12}$$

Inserting Eq. (9) into Eq. (12), we obtain nonlinear differential-difference equation:

$$i\hbar\dot{\mu}_n=S\sum_m J(n,m)\frac{[\mu_n-\eta\mu_m+\eta\mu_n^2\mu_m^*-\mu_n|\mu_m|^2]}{1+|\mu_m|^2}. \tag{13}$$

This is a modified version of the nonlinear Schrödinger equation,[32] in which intrinsic nonlinearity of the spin system has been included to all orders. However, corrections to the saddle-point approximation by considering quantum fluctuations around the stationary point would be required when we consider the case $S=1/2$, because this approximation works better for $S\gg1$.

III. NONLINEAR EIGENVALUE EQUATIONS FOR STATIONARY SELF-LOCALIZED MODES WITH A FIXED MAGNETIC HOLE

Let us seek the stationary mode solutions to Eq. (13). As an illustration, we first consider a pure 2D ferromagnet with nearest-neighbor coupling constant $J(n,m)=J$ for all n and m. This amounts to seeking the solution in the form

$$\mu_n=\frac{A}{\sqrt{2S}}\xi(\boldsymbol{n})\exp(-i\omega t), \tag{14}$$

where the quantities ω and $\xi(\boldsymbol{n})$'s are the eigenfrequency of the stationary modes to be studied and the envelope functions which are scaled by the amplitude $A/\sqrt{2S}$ and assumed to be time independent, respectively. Then substituting Eq. (14) into Eq. (13) leads to

$$\varepsilon\xi(\boldsymbol{n})-\frac{1}{2}\sum_j[\xi(\boldsymbol{n}+\boldsymbol{e}_j)+\xi(\boldsymbol{n}-\boldsymbol{e}_j)]=\frac{\lambda}{2\eta}\mathcal{U}(\xi(\boldsymbol{n})), \tag{15}$$

where

$$\varepsilon\equiv\frac{4SJ-\hbar\omega}{2\eta SJ} \tag{16}$$

and

$$\mathcal{U}(\xi(\boldsymbol{n}))=\sum_j\left[\frac{2\xi(\boldsymbol{n})\xi(\boldsymbol{n}+\boldsymbol{e}_j)^2-\eta\{\xi(\boldsymbol{n})^2\xi(\boldsymbol{n}+\boldsymbol{e}_j)+\xi(\boldsymbol{n}+\boldsymbol{e}_j)^3\}}{1+\lambda\xi(\boldsymbol{n}+\boldsymbol{e}_j)^2}+\frac{2\xi(\boldsymbol{n})\xi(\boldsymbol{n}-\boldsymbol{e}_j)^2-\eta\{\xi(\boldsymbol{n})^2\xi(\boldsymbol{n}-\boldsymbol{e}_j)+\xi(\boldsymbol{n}-\boldsymbol{e}_j)^3\}}{1+\lambda\xi(\boldsymbol{n}-\boldsymbol{e}_j)^2}\right]. \tag{17}$$

Here, the parameter λ defined by

$$\lambda\equiv A^2/2S \tag{18}$$

characterizes the nonlinearity of the spin system.

We are now concerned with stationary nonlinear modes in a 2D ferromagnet containing a hole. As a preliminary step for obtaining nonlinear lattice equations for this case, we consider a 2D ferromagnet containing an impurity spin located at the origin $\boldsymbol{n}=0$. As shown in Fig. 1, there exist two kinds of coupling constants:

$$J(m,n)=J(n,m)=\begin{cases}J' & \text{if} \quad n=0 \quad \text{and} \quad m=\pm e_j,\\ J & \text{otherwise}\end{cases} \tag{19}$$

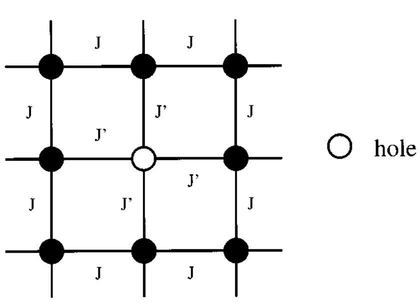

FIG. 1. Ferromagnetic system with a hole fixed at the origin.

where the exchange interaction J' between an impurity at the origin and its nearest-neighbor sites differ from J among host spin sites. When nonlinear effect is discarded, combining Eq. (19) with Eq. (15) gives

(i) for $\boldsymbol{n}=\boldsymbol{0}$,

$$\varepsilon\xi(\boldsymbol{0})-\frac{1}{2}\sum_{j=1}^{2}[\xi(\boldsymbol{e}_j)+\xi(-\boldsymbol{e}_j)]=W(\xi(\boldsymbol{0})); \tag{20}$$

(ii) for $\boldsymbol{n}=\pm\boldsymbol{e}_j$,

$$\varepsilon\xi(\pm\boldsymbol{e}_j)-\frac{1}{2}\sum_{j'=1}^{2}[\xi(\pm\boldsymbol{e}_j+\boldsymbol{e}_{j'})+\xi(\pm\boldsymbol{e}_j-\boldsymbol{e}_{j'})]=W(\xi(\pm\boldsymbol{e}_j)), \tag{21}$$

where

$$W(\xi(\boldsymbol{0}))=\left(\frac{2}{\eta}\xi(\boldsymbol{0})-\frac{1}{2}\sum_j[\xi(\boldsymbol{e}_j)+\xi(-\boldsymbol{e}_j)]\right)\frac{\Delta J}{J}, \tag{22}$$

$$W(\xi(\pm\boldsymbol{e}_j))=\left(\frac{1}{2\eta}\xi(\pm\boldsymbol{e}_j)+\frac{1}{2}\xi(\boldsymbol{0})\right)\frac{\Delta J}{J}, \tag{23}$$

with

$$\Delta J=J-J'; \tag{24}$$

(iii) for other cases,

$$\varepsilon\xi(\boldsymbol{n})-\frac{1}{2}\sum_j[\xi(\boldsymbol{n}+\boldsymbol{e}_j)+\xi(\boldsymbol{n}-\boldsymbol{e}_j)]=0. \tag{25}$$

It is understood that we eventually take the limit $J'\to 0$ to get the magnetic system with the hole. In such a case Eqs. (22) and (23) take the form

$$W(\xi(\boldsymbol{0}))=\frac{2}{\eta}\xi(\boldsymbol{0})-\frac{1}{2}\sum_{j=1}^{2}[\xi(\boldsymbol{e}_j)+\xi(-\boldsymbol{e}_j)], \tag{26}$$

$$W(\xi(\pm\boldsymbol{e}_j))=\frac{1}{2\eta}\xi(\pm\boldsymbol{e}_j)+\frac{1}{2}\xi(\boldsymbol{0}). \tag{27}$$

Our objective of obtaining stationary mode in the 2D ferromagnet with a hole can be achieved by introducing two linear operators L_0 and L':

$$L_0\xi(\boldsymbol{n})\equiv\varepsilon\xi(\boldsymbol{n})-\frac{1}{2}\sum_{j=1}^{2}[\xi(\boldsymbol{n}+\boldsymbol{e}_j)+\xi(\boldsymbol{n}-\boldsymbol{e}_j)] \tag{28}$$

with

$$E=\hbar\omega \tag{29}$$

and

$$L'\xi(\boldsymbol{n})\equiv W(\xi(\boldsymbol{n})). \tag{30}$$

Namely, L_0 is the operator for pure lattice and L' is the perturbation term due to the existence of a hole. By using these operators a generalized-version of Eq. (15) takes in the form

$$(L_0 - L')\xi(\boldsymbol{n}) = \frac{\lambda}{2\eta}\mathcal{U}(\xi(\boldsymbol{n})). \tag{31}$$

We observe that the effect of the hole and intrinsic nonlinearity of magnon excitations are incorporated into the factors L' and $(\lambda/2\eta)\mathcal{U}[\xi(\boldsymbol{n})]$. In studying solution to Eqs. (31), we introduce a magnon Green's function $g(\boldsymbol{n})$ associated with linear magnons of the pure system defined by

$$L_0 g(\boldsymbol{n}) = \varepsilon g(\boldsymbol{n}) - \frac{1}{2}\sum_{j=1}^{2}[g(\boldsymbol{n}+\boldsymbol{e}_j) + g(\boldsymbol{n}-\boldsymbol{e}_j)] = \Delta(\boldsymbol{n}). \tag{32}$$

Symbolically, $g(\boldsymbol{n})$ is written as

$$g(\boldsymbol{n}) = L_0^{-1}. \tag{33}$$

An explicit expression for $g(\boldsymbol{n})$ takes the form

$$g(\boldsymbol{n}) = \frac{1}{N}\sum_{\boldsymbol{q}} \frac{e^{i\boldsymbol{q}\cdot\boldsymbol{n}}}{\varepsilon - \sum_j \cos(q_j e_j)}. \tag{34}$$

The quantity $g(\boldsymbol{n})$ can be reduced, after lengthy, but straightforward, calculations:

$$g(\boldsymbol{n}) = g(-\boldsymbol{n}) = \int_0^\infty dt\, e^{-\varepsilon t} I_{n_1}(t) I_{n_2}(t), \tag{35}$$

where I's are Bessel functions of imaginary argument. The eigenvalue $E^{(lsw)}(\equiv \hbar\omega)$ of the linear spin-wave spectrum for the pure system is determined by the equation

$$\varepsilon - (\cos q_x + \cos q_y) = 0. \tag{36}$$

Inserting Eq. (16) into Eq. (36), the bottom of the spin energy band $E_0^{(lsw)}$ is obtained as follows:

$$\frac{E_0^{(lsw)}}{4SJ} = 1 - \eta. \tag{37}$$

From the definition of the Green's function [cf. Eq. (32)], the envelope function of linear localized mode arising from a magnetic hole is described as

$$\begin{aligned} \xi(\boldsymbol{n}) &= \sum_{\boldsymbol{l}} g(\boldsymbol{n}-\boldsymbol{l}) W(\xi(\boldsymbol{l})), \\ &= g(\boldsymbol{n}) W(\xi(\boldsymbol{0})) + \sum_j g(\boldsymbol{n}-\boldsymbol{e}_j) W(\xi(\boldsymbol{e}_j)) \\ &\quad + g(\boldsymbol{n}+\boldsymbol{e}_j) W(\xi(-\boldsymbol{e}_j)). \end{aligned} \tag{38}$$

For the present case, an s-like mode having the following symmetry with respect to the origin is physically acceptable:

$$\xi(\boldsymbol{e}_1) = \xi(-\boldsymbol{e}_1) = \xi(\boldsymbol{e}_2) = \xi(-\boldsymbol{e}_2). \tag{39}$$

Thus the following symmetric relation is also derived from Eq. (17):

$$\mathcal{U}(\xi(\boldsymbol{n})) = \mathcal{U}(\xi(-\boldsymbol{n})). \tag{40}$$

Based on this s-like mode assumption, Eq. (38) yields the compact matrix form equation

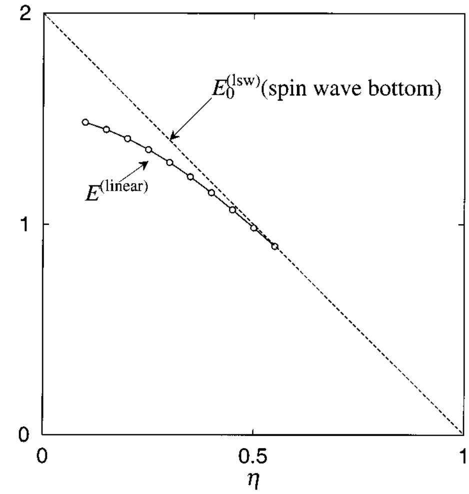

FIG. 2. η dependence of the energy eigenvalue $E^{(linear)}$ for linear localized mode with the hole effect. This eigenvalue is lying below spin-wave bottom $E_0^{(lsw)}$ without hole effect.

$$D\begin{bmatrix} \xi(\boldsymbol{0}) \\ \xi(\boldsymbol{e}_1) \end{bmatrix} = \begin{bmatrix} 0 \\ 0 \end{bmatrix}, \tag{41}$$

where

$$D = \begin{bmatrix} 1 - \frac{2}{\eta} g(\boldsymbol{0}) + 2g(\boldsymbol{e}_1) & 2g(\boldsymbol{0}) - \frac{2}{\eta} g(\boldsymbol{e}_1) \\ -\frac{2}{\eta} g(\boldsymbol{e}_1) + g(\boldsymbol{e}_1)\varepsilon & 1 + 2g(\boldsymbol{e}_1) - \frac{\varepsilon}{\eta} g(\boldsymbol{e}_1) \end{bmatrix}. \tag{42}$$

Thus the energy eigenvalue $E^{(linear)}$ of linear localized mode with the hole effect is generated by determinantal equation $\|D\| = 0$:

$$(2\eta - \varepsilon) g(\boldsymbol{0}) + 1 = 0. \tag{43}$$

The value of $E^{(linear)}$ is obtained numerically and its η dependence is plotted in Fig. 2. We recognize low lying $E^{(linear)}$ $(< E_0^{(lsw)})$, and increments of mutual energy gap with decreasing η, i.e., the system tends to the Ising type. Thus the self-localized mode can be identified due to the lowering of energy level for existence of a hole even though the system is linear.

So far our treatment is limited with the linear localized mode. We are now at the position to seek their nonlinear effect. Here, we introduce another two-site-dependent magnon Green's function $G(\boldsymbol{n};\boldsymbol{m})$, which satisfies the following equation:

$$(L_0 - L') G(\boldsymbol{n};\boldsymbol{m}) = \Delta(\boldsymbol{m}). \tag{44}$$

By using the same procedure as before, the envelope function of nonlinear self-localized mode is expressed in terms of these G's as

$$\xi(\boldsymbol{n}) = \frac{\lambda}{2\eta}\sum_{m} G(\boldsymbol{n};\boldsymbol{m})\mathcal{U}(\xi(\boldsymbol{m})). \tag{45}$$

Equation (44) yields the Green's function $G(\boldsymbol{n};\boldsymbol{m})$ to be

$$G(\boldsymbol{n};\boldsymbol{m})=L_0^{-1}+L_0^{-1}L'G(\boldsymbol{n};\boldsymbol{m})$$
$$=L_0^{-1}+\sum_{\boldsymbol{l}} L_0^{-1}W(G(\boldsymbol{l};\boldsymbol{m})), \tag{46}$$

where

$$W(G(\boldsymbol{0};\boldsymbol{m}))=\frac{2}{\eta}G(\boldsymbol{0};\boldsymbol{m})-\frac{1}{2}\sum_j \{G(\boldsymbol{e}_j;\boldsymbol{m})+G(-\boldsymbol{e}_j;\boldsymbol{m})\}, \tag{47}$$

$$W(G(\boldsymbol{e}_j;\boldsymbol{m}))=\frac{1}{2\eta}G(\boldsymbol{e}_j;\boldsymbol{m})+\frac{1}{2}G(\boldsymbol{0};\boldsymbol{m}), \tag{48}$$

$$W(G(\boldsymbol{l};\boldsymbol{m}))=0 \quad \text{for} \quad |\boldsymbol{l}|>1. \tag{49}$$

In writing the above Eq. (46), Eq. (30) is used. Using of Eq. (33), $G(\boldsymbol{n};\boldsymbol{m})$ are written by

$$G(\boldsymbol{n};\boldsymbol{m})=g(\boldsymbol{n}-\boldsymbol{m})+\left[\frac{E}{\eta}g(\boldsymbol{n})+\Delta(\boldsymbol{n})\right]G(\boldsymbol{0};\boldsymbol{m})$$
$$+\frac{1}{2\eta}\sum_j \{[g(\boldsymbol{n}-\boldsymbol{e}_j)-\eta g(\boldsymbol{n})]G(\boldsymbol{e}_j;\boldsymbol{m})$$
$$+[g(\boldsymbol{n}+\boldsymbol{e}_j)-\eta g(\boldsymbol{n})]G(-\boldsymbol{e}_j;\boldsymbol{m})\}. \tag{50}$$

It is instructive to remark that $G(\boldsymbol{n};\boldsymbol{m})$ is dependent on sites $\boldsymbol{n}$ and $\boldsymbol{m}$ and is expressed in terms of $g(\boldsymbol{n}-\boldsymbol{m})$, $G(\boldsymbol{0};\boldsymbol{m})$, $G(\pm\boldsymbol{e}_1;\boldsymbol{m})$, and $G(\pm\boldsymbol{e}_2;\boldsymbol{m})$, while $g(\boldsymbol{n},\boldsymbol{m})=g(\boldsymbol{n}-\boldsymbol{m})$ depends only on their relative distance.

Putting $\boldsymbol{n}=\boldsymbol{0}$ and $\boldsymbol{n}=\pm\boldsymbol{e}_j$ in Eq. (50), we obtain a 5×5 matrix form equation with respect to five magnon Green's functions $G(\boldsymbol{0};\boldsymbol{m})$, $G(\pm\boldsymbol{e}_1;\boldsymbol{m})$, and $G(\pm\boldsymbol{e}_2;\boldsymbol{m})$,

$$\begin{bmatrix} g(\boldsymbol{m}) \\ g(\boldsymbol{m}-\boldsymbol{e}_1) \\ g(\boldsymbol{m}+\boldsymbol{e}_1) \\ g(\boldsymbol{m}-\boldsymbol{e}_2) \\ g(\boldsymbol{m}+\boldsymbol{e}_2) \end{bmatrix} = \begin{bmatrix} -Eg(\boldsymbol{0}) & A & A & A & A \\ C & B & D & F & F \\ C & D & B & F & F \\ C & F & F & B & D \\ C & F & F & D & B \end{bmatrix} \begin{bmatrix} G(\boldsymbol{0};\boldsymbol{m}) \\ G(\boldsymbol{e}_1;\boldsymbol{m}) \\ G(-\boldsymbol{e}_1;\boldsymbol{m}) \\ G(\boldsymbol{e}_2;\boldsymbol{m}) \\ G(-\boldsymbol{e}_2;\boldsymbol{m}) \end{bmatrix}, \tag{51}$$

where

$$A=-SJ(g(\boldsymbol{e}_1)-\eta g(\boldsymbol{0})),$$
$$B=1-SJ(g(\boldsymbol{0})-\eta g(\boldsymbol{e}_1)),$$
$$C=-Eg(\boldsymbol{e}_1),$$
$$D=-SJ(g(2\boldsymbol{e}_1)-\eta g(\boldsymbol{e}_1)),$$
$$F=-SJ(g(\boldsymbol{e}_1+\boldsymbol{e}_2)-\eta g(\boldsymbol{e}_1)).$$

Therefore these five magnon Green's functions are solved as

$$\begin{bmatrix} G(\boldsymbol{0};\boldsymbol{m}) \\ G(\boldsymbol{e}_1;\boldsymbol{m}) \\ G(-\boldsymbol{e}_1;\boldsymbol{m}) \\ G(\boldsymbol{e}_2;\boldsymbol{m}) \\ G(-\boldsymbol{e}_2;\boldsymbol{m}) \end{bmatrix} = \begin{bmatrix} -Eg(\boldsymbol{0}) & A & A & A & A \\ C & B & D & F & F \\ C & D & B & F & F \\ C & F & F & B & D \\ C & F & F & D & B \end{bmatrix}^{-1} \begin{bmatrix} g(\boldsymbol{m}) \\ g(\boldsymbol{m}-\boldsymbol{e}_1) \\ g(\boldsymbol{m}+\boldsymbol{e}_1) \\ g(\boldsymbol{m}-\boldsymbol{e}_2) \\ g(\boldsymbol{m}+\boldsymbol{e}_2) \end{bmatrix}. \tag{52}$$

Thus we can finally evaluate $G(\boldsymbol{n};\boldsymbol{m})$ for general sites $\boldsymbol{n}$ and $\boldsymbol{m}$ from Eq. (50) with Eqs. (34) and (52).

Since the profile function $\xi(\boldsymbol{n})$'s are scaled by the amplitude $A/\sqrt{2S}$ as described before, let us regard $\xi(\pm\boldsymbol{e}_j)$ as unity, which are ones at the nearest neighbors to the hole position $\boldsymbol{n}=(0,0)$. This normalization condition can be then written as

$$\xi(\pm\boldsymbol{e}_j)=\frac{\lambda}{2\eta}\sum_m G(\pm\boldsymbol{e}_j;\boldsymbol{m})\mathcal{U}(\xi(\boldsymbol{m}))=1. \tag{53}$$

As a result, Eq. (45) is rewritten as

$$\xi(\boldsymbol{n})=\frac{\sum_m G(\boldsymbol{n};\boldsymbol{m})\mathcal{U}(\xi(\boldsymbol{m}))}{\sum_m G(\boldsymbol{e}_j;\boldsymbol{m})\mathcal{U}(\xi(\boldsymbol{m}))} \quad \text{for} \quad \boldsymbol{n}\neq\boldsymbol{0}. \tag{54}$$

In seeking the relations among the energy eigenvalue E, nonlinear parameter λ, and $\xi(\boldsymbol{n})$'s, Eqs. (53) and (54) are treated numerically under the following procedure: (i) The numerical value of the anisotropy factor is chosen within $1>\eta>0$. (ii) For each value of η, the trial values λ and $\xi(\boldsymbol{n})$'s for $10\geqslant n_1\geqslant n_2\geqslant 2$ are provided. (iii) For a given parameter ε, the successive approximate calculations are performed on Eqs. (53) and (54). The numerical calculations are carried out only for $n_1\geqslant n_2\geqslant 1$, because of the symmetric properties of the s-like mode. (iv) The pth approximate solutions $\xi^p(\boldsymbol{n})$ and λ^p for $\xi(\boldsymbol{n})$ and λ, respectively, are truncated if the relative truncating error, for instance $\xi^p(\boldsymbol{n})-\xi^{p-1}(\boldsymbol{n})$, becomes less than 10^{-6}. Sufficient convergence of the successive approximation was attained at $p=15$ on the average.

In Fig. 3(a), the energy eigenvalue E of the self-localized s-like nonlinear mode is plotted against λ for various values of η. The increment of the nonlinear parameter λ brings the lowering of E. The difference $E(0)-E(\lambda)$, which indicates the nonlinear effect because $E(0)$ corresponds to that of the linear self-localized mode under hole contribution, becomes relatively large for small value of η (Ising-like). In Fig. 3(b), it is illustrated for $\eta=0.3$ how the eigenvalue E is lowered under two effects, i.e., the intrinsic nonlinearity and the extrinsic hole doping. In addition to $E_0^{(lsw)}$ and $E^{(linear)}$, the λ dependence of $E^{(pure)}(\lambda)$ is also shown there for reference, which is the energy eigenvalue for the pure system including nonlinear effect (see the Appendix). We can esti-

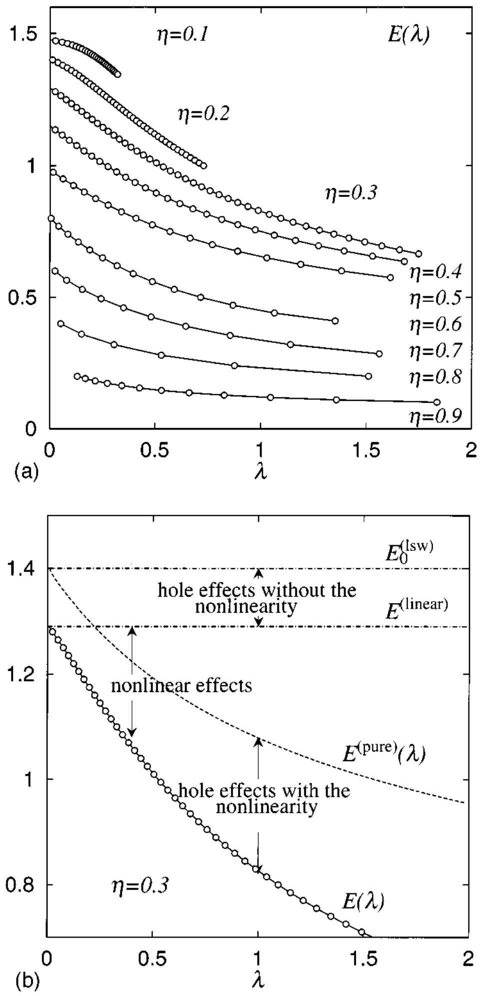

FIG. 3. (a) The energy eigenvalue $E(\lambda)$ of an s-like self-localized mode as a function of nonlinearity parameter λ for various anisotropic exchange interactions parameters. (b) Illustration of energy reduction under two effects, i.e., intrinsic nonlinearity and extrinsic hole doping in a case of $\eta=0.1$. The solid line is $E(\lambda)$ and the dashed line is the $E^{(pure)}(\lambda)$.

mate the energy reduction originated in the hole effect as $E_0^{(lsw)}-E^{(linear)}$ for the linear system $(\lambda=0)$ and $E^{(pure)}(\lambda)-E(\lambda)$ for nonlinear system, respectively. With increasing the nonlinearity parameter, the hole existence stimulates lowering of the energy E as seen in Fig. 3(b).

Since the diagonal coherent-state representation of spin operator $\boldsymbol{S}_n$ is given in terms of the profile function $\xi(\boldsymbol{n})$ as

$$\frac{\langle \mu_n|S_n^x|\mu_n\rangle}{S}=\frac{\sqrt{\lambda}\,\xi(\boldsymbol{n})}{1+\lambda\,\xi(\boldsymbol{n})^2}\cos\omega t \quad \text{and}$$

$$\frac{\langle \mu_n|S_n^y|\mu_n\rangle}{S}=-\frac{\sqrt{\lambda}\,\xi(\boldsymbol{n})}{1+\lambda\,\xi(\boldsymbol{n})^2}\sin\omega t, \tag{55}$$

the projection of $\boldsymbol{S}_n$ on the 2D square lattice plane, denoted $\boldsymbol{S}_n^{\perp}$, can be evaluated. In Fig. 4 the obtained results are drawn for two cases, (a) $\eta=0.3$ and (b) $\eta=0.5$, with given values of λ and E. In the case of $\eta=0.3$, $\boldsymbol{S}_n^{\perp}$ appear largely in the

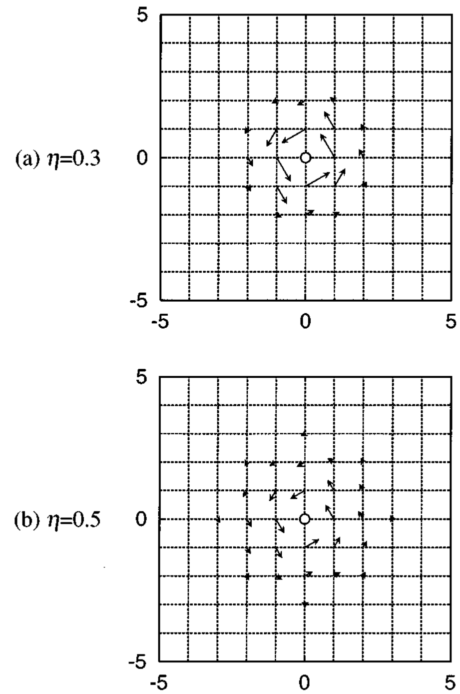

FIG. 4. The projection of spin profile of an s-like self-localized mode $\boldsymbol{S}_n$ on a xy plane. (a) $\eta=0.3$ with $E=0.90$ and $\lambda=0.58$ (b) $\eta=0.5$ with $E=0.90$ and $\lambda=0.10$.

magnitude around a hole site $\boldsymbol{n}=\boldsymbol{0}$ with the direction indicated by arrows. Thus we find a localized magnetic vortex. This implies that spins in the neighborhood of a hole undergo a large excursion, while the deviation from ferromagnetic state is very small for rest ones. This localized magnetic vortex seems to be a peculiarity in 2D nonlinear spin systems associated with a hole, and is in contrast with the spin-wave case, in which $\boldsymbol{S}_n^{\perp}$ propagates over all lattice sites. As the system shifts to the Heisenberg type, the vortex region spreads out surrounding the hole but the magnitudes of $\boldsymbol{S}_n^{\perp}$ become smaller than the former case, as shown in Fig. 4(b).

IV. TIME EVOLUTION FOR MOVING NONLINEAR SELF-LOCALIZED MAGNONS

In this section we discuss the time evolution for the moving nonlinear self-localized magnons, with particular attention to interplaying between the intrinsic nonlinearity and the structural disorder due to the existence of a hole. We look for solutions to Eq. (13) in the form

$$\mu_n=|\mu_n|\exp(i\theta_n)\equiv\frac{A}{\sqrt{2S}}\chi(\boldsymbol{n})\exp(i\theta_n), \tag{56}$$

where the quantities $\chi(\boldsymbol{n})$ and θ_n are time-dependent envelope function for the complex field variable μ_n and its phase factor, respectively. Thus it reduces to

$$i\hbar\dot{\chi}(\boldsymbol{n})-\hbar\dot{\theta}_n\chi(\boldsymbol{n})=SJ\sum_m \frac{\chi(\boldsymbol{n})[1-\lambda\chi(\boldsymbol{m})^2]-\eta\chi(\boldsymbol{m})\{\exp[i(\theta_m-\theta_n)]-\lambda\chi(\boldsymbol{n})^2\exp[-i(\theta_m-\theta_n)]\}}{1+\lambda\chi(\boldsymbol{m})^2}. \tag{57}$$

We take the phase factor θ_n to be of the form

$$\theta_n=\boldsymbol{k}\cdot\boldsymbol{n}-\omega t+\alpha_n. \tag{58}$$

The quantity $\boldsymbol{k}$ is not a so-called wave vector but should be treated as a parametric vector, because the periodicity of the system with a magnetic hole is not allowed, and the quantity of α_n is a phase-shift function. Insertion of Eq. (58) into Eq. (57) leads to a pair of equations:

$$\hbar\dot{\chi}(\boldsymbol{n})=-\eta SJ[1+\lambda\chi(\boldsymbol{n})^2]\times\sum_j\left(\sin[k_j+\alpha(\boldsymbol{n}+\boldsymbol{e}_j)-\alpha(\boldsymbol{n})]\frac{\chi(\boldsymbol{n}+\boldsymbol{e}_j)}{1+\lambda\chi(\boldsymbol{n}+\boldsymbol{e}_j)^2}-\sin[k_j+\alpha(\boldsymbol{n})-\alpha(\boldsymbol{n}-\boldsymbol{e}_j)]\frac{\chi(\boldsymbol{n}-\boldsymbol{e}_j)}{1+\lambda\chi(\boldsymbol{n}-\boldsymbol{e}_j)^2}\right), \tag{59}$$

and

$$\hbar\omega\chi(\boldsymbol{n})-\hbar\dot{\alpha}(\boldsymbol{n})\chi(\boldsymbol{n})=SJ\sum_j\left[\left(\frac{1-\lambda\chi(\boldsymbol{n}+\boldsymbol{e}_j)^2}{1+\lambda\chi(\boldsymbol{n}+\boldsymbol{e}_j)^2}+\frac{1-\lambda\chi(\boldsymbol{n}-\boldsymbol{e}_j)^2}{1+\lambda\chi(\boldsymbol{n}-\boldsymbol{e}_j)^2}\right)\chi(\boldsymbol{n})-\eta[1-\lambda\chi(\boldsymbol{n})^2]\left(\cos[k_j+\alpha(\boldsymbol{n}+\boldsymbol{e}_j)-\alpha(\boldsymbol{n})]\times\frac{\chi(\boldsymbol{n}+\boldsymbol{e}_j)}{1+\lambda\chi(\boldsymbol{n}+\boldsymbol{e}_j)^2}+\cos[k_j+\alpha(\boldsymbol{n})-\alpha(\boldsymbol{n}-\boldsymbol{e}_j)]\times\frac{\chi(\boldsymbol{n}-\boldsymbol{e}_j)}{1+\lambda\chi(\boldsymbol{n}-\boldsymbol{e}_j)^2}\right)\right]. \tag{60}$$

Equations (59) and (60), which are to be treated simultaneously, do not appear exactly solvable. The former describes the time evolution of the self-localized magnon mode, and the latter determines its eigenfrequancy, if α_n's are slowly varying with respect to time. With the assumption of $\dot{\alpha}_n\simeq 0$, Eq. (60) is rewritten

$$\varepsilon\chi(\boldsymbol{n})-\frac{1}{2}\sum_j\cos(k_j)[\chi(\boldsymbol{n}+\boldsymbol{e}_j)+\chi(\boldsymbol{n}-\boldsymbol{e}_j)]=\frac{\lambda}{2\eta}\mathcal{U}(\chi(\boldsymbol{n})), \tag{61}$$

where

$$\mathcal{U}(\chi(\boldsymbol{n}))=\sum_j\left[\left(\frac{2\chi(\boldsymbol{n})\chi(\boldsymbol{n}+\boldsymbol{e}_j)^2}{1+\lambda\chi(\boldsymbol{n}+\boldsymbol{e}_j)^2}+\frac{2\chi(\boldsymbol{n})\chi(\boldsymbol{n}-\boldsymbol{e}_j)^2}{1+\lambda\chi(\boldsymbol{n}-\boldsymbol{e}_j)^2}\right)-\eta\left(\cos[k_j+\alpha(\boldsymbol{n}+\boldsymbol{e}_j)-\alpha(\boldsymbol{n})]\times\frac{\chi(\boldsymbol{n})^2\chi(\boldsymbol{n}+\boldsymbol{e}_j)+\chi(\boldsymbol{n}+\boldsymbol{e}_j)^3}{1+\lambda\chi(\boldsymbol{n}+\boldsymbol{e}_j)^2}+\cos[k_j+\alpha(\boldsymbol{n})-\alpha(\boldsymbol{n}-\boldsymbol{e}_j)]\frac{\chi(\boldsymbol{n})^2\chi(\boldsymbol{n}-\boldsymbol{e}_j)+\chi(\boldsymbol{n}-\boldsymbol{e}_j)^3}{1+\lambda\chi(\boldsymbol{n}-\boldsymbol{e}_j)^2}-\frac{\sin(k_j)}{\lambda}\{[\alpha(\boldsymbol{n}+\boldsymbol{e}_j)-\alpha(\boldsymbol{n})]\chi(\boldsymbol{n}+\boldsymbol{e}_j)+[\alpha(\boldsymbol{n})-\alpha(\boldsymbol{n}-\boldsymbol{e}_j)]\chi(\boldsymbol{n}-\boldsymbol{e}_j)\}\right)\right]. \tag{62}$$

Equation (61) reduces to Eq. (15) when $\boldsymbol{k}=0$ and $\alpha_n=0$. The initial phase α_n's are determined by energy minimization condition $\partial\omega/\partial\alpha_n=0$:

$$\sum_j \sin[k_j+\alpha(\boldsymbol{n}+\boldsymbol{e}_j)-\alpha(\boldsymbol{n})]\frac{\chi(\boldsymbol{n}+\boldsymbol{e}_j)}{1+\lambda\chi(\boldsymbol{n}+\boldsymbol{e}_j)^2}=\sin[k_j+\alpha(\boldsymbol{n})-\alpha(\boldsymbol{n}-\boldsymbol{e}_j)]\frac{\chi(\boldsymbol{n}-\boldsymbol{e}_j)}{1+\lambda\chi(\boldsymbol{n}-\boldsymbol{e}_j)^2}. \tag{63}$$

Since the mathematical scheme of Eq. (61) is completely the same as that of Eq. (15), except for involving constant factors $\cos(k_j)$ and α's determined by Eq. (63), it can be solved under the same procedure for treatment of Eq. (15). After lengthy, but straightforward, numerical calculation, the *s*-like self-localized nonlinear mode is obtained for arbitrary $\boldsymbol{k}$ value, and we used it as the initial state for its time evolution.

For the equation of motion of $\chi(\boldsymbol{n})$ in Eq. (59), numerical analysis is performed by using Runge-Kutta-Jill method.[26] The time evolution of the profile of the self-localized mode with $k_1=k_2=0.1$ is shown for the system with $\eta=0.1$ in Fig. 5(a) and $\eta=0.5$ in Fig. 5(b), respectively. The propagation of a moving localized mode leaving behind the fixed localized mode in the neighborhood of a hole site is observed in both cases. Namely, we can see two kinds of localized modes, one is intrinsic due to the nonlinearity, being in principle mobile, and the other is extrinsic due to the hole, being immobile. As the anisotropy parameter η decreases, i.e., it becomes Ising-like, they are more separable from each other for the same elapsed time, because the intrinsic nonlinear self-localized mode propagates with getting trapped at a particular lattice site, i.e., its locality becomes stronger for smaller values of η. In contrast with this case, with increas-

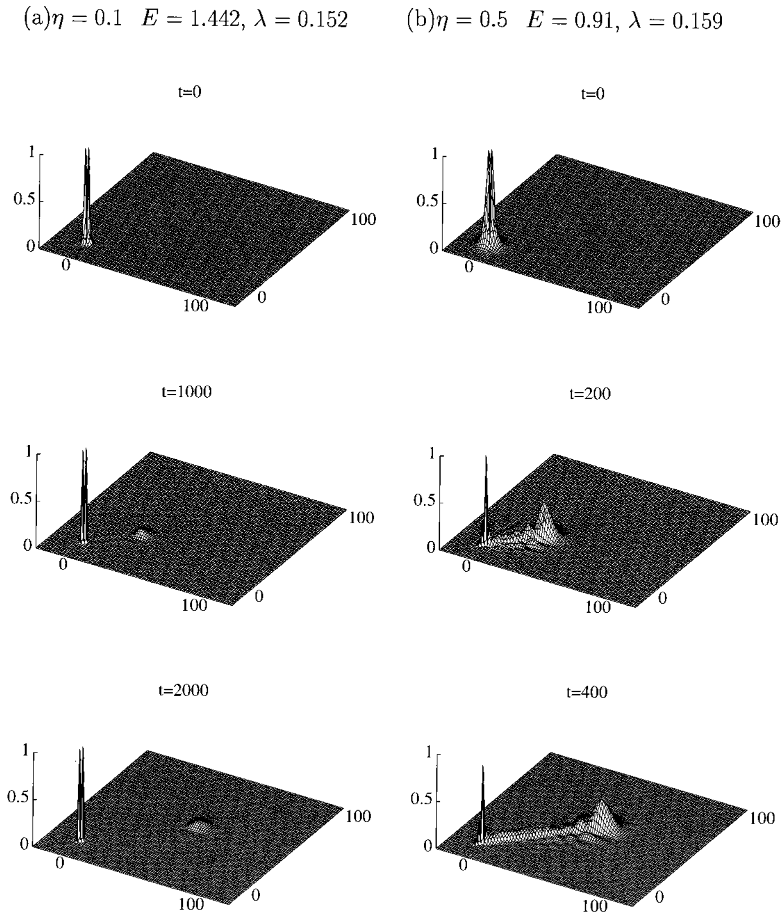

FIG. 5. The time evolution of the self-localized magnon mode for $k_x = k_y = 0.1$. (a) $\eta = 0.1$ with $E = 1.442$, $\lambda = 0.152$ at time is 0, 1000, 2000 and (b) $\eta = 0.5$ with $E = 0.91$, $\lambda = 0.159$ at time is 0, 200, 400.

ing η the interplaying of the moving localized mode and the fixed localized mode becomes important. As shown in Fig. 5(b), the former propagates with keeping the effect of the latter along a line connecting them. Within these areas the ferromagnetism is locally destroyed.

These situations are confirmed by comparison with that of the pure system without hole effect. For reference, the profiles of the self-localized modes $\chi_p(\boldsymbol{n})$ for the pure case are illustrated in Figs. 6(a) and 6(b) with the same η parameters, to Figs. 5(a) and 5(b), respectively. We observe there larger the propagating velocity of $\chi_p(\boldsymbol{n})$ and wider spread out region of $\chi_p(\boldsymbol{n}) \neq 0$ for larger values of η, i.e., the intrinsic nonlinear self-modes are delocalized as $\eta \rightarrow 1$. This moving localized mode, however, becomes unstable during the entire time interval because of nonintegrability of the system and collapse in the spin-wave mode.

V. CONCLUDING REMARKS

Previously, we formulated a $SU(2)$ coherent-state path-integral theory of collective mode in one-dimensional anisotropic Heisenberg ferromagnets[16] not only for stationary modes but also moving ones. In this paper we extend this theory to two dimensional spatially inhomogeneous ferromagnetic cases, i.e., with doping a fixed hole. A stationary-phase approximation[29] is employed to derive nonlinear differential-difference equation for collective mode with no assumption on the smallness of spin deviation from the ferromagnetic state and full inclusion of the intrinsic nonlinearity in magnon system. The formulation given here leads to a natural extension of the conventional spin-wave theory to nonlinear regime, where wavelike magnons are modulated by the intrinsic nonlinearity into particlelike self-localized magnons.

Stationary nonlinear self-localized magnons are investigated by introducing two kinds of magnon Green's functions, $g(\boldsymbol{n}-\boldsymbol{m})$ and $G(\boldsymbol{n};\boldsymbol{m})$, which are defined in the linear system. The former is associated with pure system, and the latter is related to a hole existence and rather complicated dependence on two sites $\boldsymbol{n}$ and $\boldsymbol{m}$. Using the analytical properties of these Green's functions, the formal expressions of the profile functions of the stationary nonlinear self-localized modes are obtained in the spatially inhomogeneous system. Concretely, numerical calculations are made for the *s*-like mode having the symmetry respect to the hole position, and a magnetic vortex is found.

As is well known, if nonmagnetic ions exist in the system, the localized mode appears in spite of a linear system,[1–7] and the energy eigenvalue is reduced below that of linear spin wave. In the present nonlinear system, such energy reduction is enhanced in cooperation with the intrinsic nonlinearity. This tendency becomes more prominent for smaller anisotropic parameter η (Ising-like). Thus the profile function is expected to be trapped at a few particular lattice sites, i.e., localized strongly as $\eta \rightarrow 0$. Looking at the projection onto x-y components of spin, it takes vortex shape in the neighborhood of a hole, as shown in Figs. 4(a) and 4(b). We find its size decreases as $\eta \rightarrow 0$, but the deviations from the ferromagnetic state become large as denoted by arrows. This

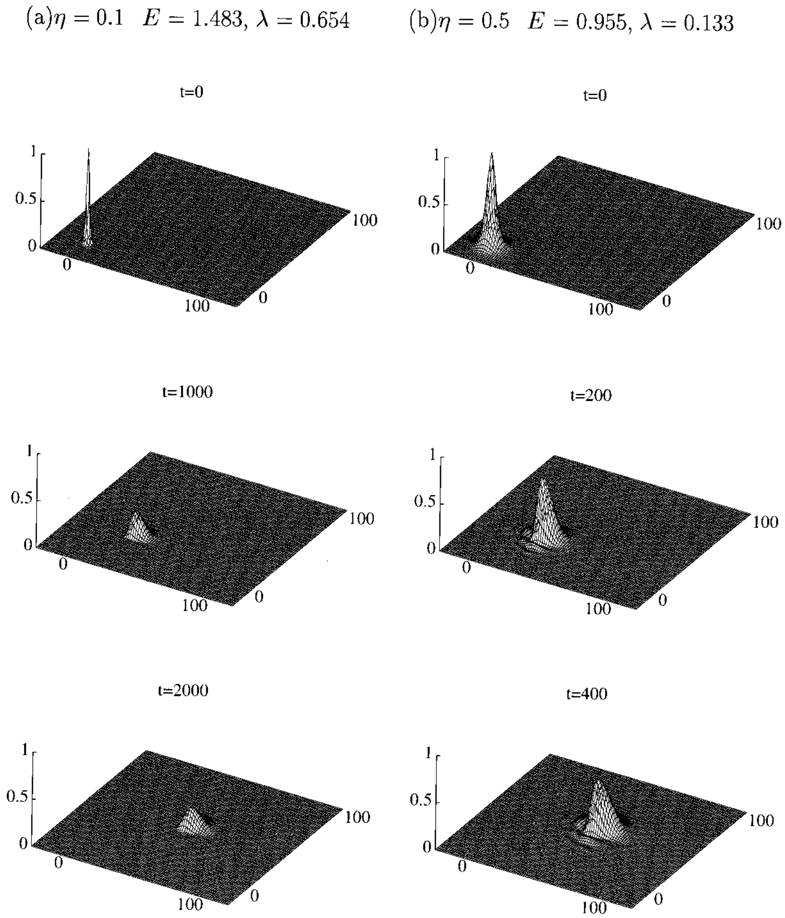

FIG. 6. The time evolution of the self-localized magnon mode $\xi_p(t,\boldsymbol{n})$ for $k_x = k_y = 0.1$ in pure lattice. (a) $\eta = 0.1$ with $E = 1483$ and $\lambda = 0.654$ at time is 0, 1000, 2000 and (b) $\eta = 0.5$ with $E = 0.955$ and $\lambda = 0.133$ at time is 0, 200, 400.

implies the ferromagnetism is suppressed strongly but locally.

The time evolution for the nonlinear self-localized magnon is discussed with emphasis on interplaying between the intrinsic nonlinearity and the extrinsic hole existence. We find the propagation of a moving localized mode leaving behind the fixed localized mode in the neighborhood of a hole. By comparison with the time evolution of nonlinear localized mode for the pure system it is interpreted as that the former is due to the nonlinearity, being, in principle, mobile, and the latter is due to the hole doping and immobile. As the anisotropy parameter η decreases, the moving localized mode is more separable from the fixed ones for the same elapsed time, because the self-localized mode is solidified as described above. In contrast to so called magnetic soliton, the localized mode however becomes unstable during the entire time interval as shown in Figs. 5 and 6. This feature is attributed to the nonintegrable property of the considered discrete lattice, i.e., the moving localized mode collapses in the magnon modes.[24]

Before closing this section, it is worthwhile to mention that (i) although the concept of the intrinsic nonlinear localized mode is established so far,[8–23] it has been scarcely reported from experimental side related to these subjects. So, it is demanded urgently to observe this kind of localized mode by means of the infrared-absorption measurements,[33] etc. (ii) Under a similar treatment, we can analyze the localized mode for the antiferromagnet with a hole doping. However, to take account of quantum fluctuation the fermion coherent-state path-integral formulations[34] are useful, because one can directly treat the quantum spin system ($S = 1/2$) by this method. This might provide the important clue to the mechanism of the high-T_c superconductivity. Information regarding this point will be presented elsewhere.

APPENDIX: TIME EVOLUTION IN PERFECT SYSTEM

In a perfect system, the equation of motion for nonlinear self-localized mode $\xi_p(\boldsymbol{n})$ is obtained by omitting the perturbation term L' in Eq. (31),

$$L_0 \xi_p(\boldsymbol{n}) = \frac{\lambda}{2\eta} \mathcal{U}(\xi_p), \tag{A1}$$

where $\mathcal{U}(\xi_p(\boldsymbol{n}))$ is given in Eq. (17). The envelope function of the stationary localized mode is described in terms of the Green's function $g(\boldsymbol{n})$ defined in Eq. (33),

$$\xi_p(\boldsymbol{n}) = L_0^{-1} \frac{\lambda}{2\eta} \mathcal{U}(\xi) = \frac{\lambda}{2\eta} \sum_m g(\boldsymbol{n},\boldsymbol{m}) \mathcal{U}(\xi_p(\boldsymbol{m})). \tag{A2}$$

Equation (57) governs the time evolution of the localized mode $\chi_p(t,\boldsymbol{n})$ for the pure system too. Regarding the solution of Eq. (A2) as the initial state $\chi_p(0,\boldsymbol{n})$, numerical calculation is carried out for Eq. (57) under the similar procedure described in the text. But the boundary condition is changed here as $\chi_p(0,\boldsymbol{0}) = 1$. As a result, the time evolution $\chi_p(t,\boldsymbol{n})$ is evaluated.

[1] S. Takeno, Prog. Theor. Phys. **30**, 565 (1963); **30**, 731 (1963).
[2] T. Wolfram and J. Callaway, Phys. Rev. **130**, 2207 (1963).
[3] T. Tonegawa and J. Kanamori, Phys. Lett. **21**, 130 (1966); T. Tonegawa, Prog. Theor. Phys. **40**, 1195 (1969).
[4] S. W. Lovesey, J. Phys. C **1**, 102 (1968); **1**, 118 (1968).
[5] S. Takeno, Prog. Theor. Phys. **28**, 33 (1962).
[6] For a review of theory, see A. A. Maradudin, E. W. Montroll, G. H. Weiss, and I. P. Ipatova, *Theory of Lattice Dynamics in the Harmonic Approximation, Solid State Physics, Suppl. 3*, 2nd ed. (Academic Press, New York, 1971).
[7] For a review of theory, see A. S. Baker and A. J. Sievers, Rev. Mod. Phys. **47**, 1 (1975).
[8] A. S. Dolgov, Fiz. Tverd. Tela (Leningrad) **28**, 1641 (1986) [Sov. Phys. Solid State **28**, 907 (1986)].
[9] A. J. Sievers and S. Takeno, Phys. Rev. Lett. **61**, 970 (1988).
[10] S. Takeno and A. J. Sievers, Solid State Commun. **67**, 1023 (1988).
[11] S. Takeno, K. Kisoda, and A. J. Sievers, Prog. Theor. Phys. Suppl. **94**, 242 (1988).
[12] V. M. Burlakov, S. A. Kiselev, and V. N. Pyrkov, Phys. Rev. B **42**, 4921 (1990).
[13] J. B. Page, Phys. Rev. B **41**, 7835 (1990).
[14] S. Takeno and K. Kawasaki, Phys. Rev. B **45**, R5083 (1992).
[15] S. Takeno and K. Kawasaki, J. Phys. Soc. Jpn. **61**, 4547 (1992).
[16] S. Takeno and K. Kawasaki, J. Phys. Soc. Jpn. **63**, 1928 (1994).
[17] R. F. Wallis, D. L. Mills, and A. D. Boardman, Phys. Rev. B **52**, R3828 (1995).
[18] S. Rakhmanova and D. L. Mills, Phys. Rev. B **54**, 9225 (1996).
[19] R. Lai, S. A. Kiselev, and A. J. Sievers, Phys. Rev. B **54**, R12 665 (1996).
[20] R. Lai and A. J. Sievers, Phys. Rev. B **55**, R11 937 (1997).
[21] J. Ohishi, M. Kubota, K. Kawasaki, and S. Takeno, Phys. Rev. B **55**, 8812 (1997).
[22] R. Lai, S. A. Kiselev, and A. J. Sievers, Phys. Rev. B **56**, 5345 (1997).
[23] S. Takeno, M. Kubota, and K. Kawasaki, Physica D **113**, 366 (1998).
[24] R. Lai and A. J. Sievers, Phys. Rev. B **57**, 3433 (1998).
[25] J. G. Bednorz and K. A. Müller, Z. Phys. B **64**, 189 (1986).
[26] J. R. Rice, *Numerical Methods, Software and Analysis* (McGraw-Hill, New York, 1983).
[27] A. M. Perelomov, *Generalized Coherent States and Their Applications* (Springer-Verlag, Berlin, 1986).
[28] J. M. Radcliffe, J. Phys. A **4**, 313 (1971).
[29] H. Kuratsuji and T. Suzuki, J. Math. Phys. **21**, 472 (1980).
[30] R. P. Feynman and A. R. Hibbs, *Quantum Mechanics and Path Integrals* (McGraw-Hill, New York, 1965).
[31] J. R. Klauder and B. S. Skagerstam, *Coherent States. Applications in Physics and Mathematical Physics* (World Scientific, Singapore, 1985).
[32] R. K. Dodd, J. C. Eilbeck, J. D. Gibbon, and H. C. Morris, *Solitons and Nonlinear Wave Equations* (Academic Press, London, 1982).
[33] Very recently, one of the present authors (S.T.) was informed that Sievers and his co-workers succeeded in identifying intrinsic nonlinear localized modes in antiferromagnets. U. T. Schwarz, L. Q. English, and A. J. Sievers, Phys. Rev. Lett. **83**, 223 (1999).
[34] K. Moulopoulos and N. W. Ashcroft, Phys. Rev. Lett. **66**, 2915 (1991).